Isotopic fractionation in the proto-lunar disk: constraints on equilibration

Kaveh Pahlevan[1*], Charles Gammie[2]

1. School of Earth and Space Exploration, Arizona State University, Tempe, AZ, 85281
2. Department of Astronomy, University of Illinois, 1002 West Green Street, Urbana, IL, 61801

*To whom correspondence should be addressed:

Email: kaveh.pahlevan@asu.edu

Tel: +1 (480) 401 8584

Fax: +1 (480) 965 8102

5 Figures

Submitted to EPSL

Abstract

Despite its importance to questions of lunar origin, the evolution of the proto-lunar disk has eluded a precise description. A number of recent developments have nevertheless made it possible to constrain this evolution. Here, we use a physical-chemical model of the proto-lunar disk with a silicate vapor atmosphere and a separately convective magma layer to explore the consequences of turbulent mixing across the radial extent of the disk. Four features of such a stratified turbulent disk act in concert to radially separate the isotopes (e.g. of silicon) by mass: (i) the melt-vapor interface exhibits a temperature gradient across the radial extent of the disk, (ii) silicon exists as SiO_4^{-4} in the melt and primarily as SiO in the co-existing vapor, with the difference in bonding environment resulting in relatively large equilibrium isotopic fractionation (~0.5 per mil difference in $^{30}Si/^{28}Si$) between the two phases, (iii) thermodynamic equilibrium between a magma layer and a co-existing atmosphere – if attained – will therefore tend to concentrate the heavy isotopes into the magma layer, generating an atmosphere that is isotopically light, with the magnitude of isotopic difference dependent on temperature. Radial temperature gradients will, in this way, be translated – through equilibrium partitioning – to gradients in the isotopic composition of the magma layer and the complementary atmosphere, and (iv) turbulent radial mixing in the atmosphere will therefore result in radial isotopic transport, which, in the case of silicon, would tend to concentrate the heavy (light) isotopes in the outer (inner) regions of the disk. That the inner disk material accretes back onto the Earth while the outer disk participates in lunar accretion permits such a redistribution process to be expressed in the isotopic composition of the silicate Earth and Moon. The current precision with which the silicon isotopic composition of these reservoirs is known constrains the degree to which the proto-lunar disk could have existed in such a stratified diffusive regime. These results suggest that – if post-impact Earth-disk equilibration is the cause of the

remarkable isotopic homogeneity observed in the Earth-Moon system – the liquid in the proto-lunar disk must have been entrained into the overlying convective atmosphere and have participated in the turbulent mixing process. Consequences for the post-impact evolution are discussed.

Keywords: Moon, origin, proto-lunar disk, equilibration, isotopes

1. Introduction

The Moon is generally thought to have formed from a melt-vapor disk generated via the off-center impact of a planet-sized body with the proto-Earth towards the end of Earth accretion (Cameron and Ward, 1976; Hartmann and Davis, 1975). Such an origin via giant impact can explain the angular momentum present in the Earth-Moon (EM) system (Cameron and Ward, 1976), the lunar mass and Fe deficit (Canup and Asphaug, 2001), and the small but non-zero inclination of the lunar orbit (Ćuk et al., 2016; Pahlevan and Morbidelli, 2015; Touma and Wisdom, 1998; Ward and Canup, 2000). In its simplest formulation, however, the giant impact model cannot readily explain the precise isotopic similarities observed between the silicate Earth and Moon (Kruijer and Kleine, 2017; Pahlevan, 2014) as most of the material that is injected into orbit is sourced from the impacting planet rather than the proto-Earth, a robust feature seen in all simulations of impacts that leave the system with its current level of angular momentum (Canup, 2004; Canup and Asphaug, 2001; Canup et al., 2013). Here, we refer to the low-velocity, oblique, Mars-mass impact onto the proto-Earth as the "standard" impact.

Motivated by the problem of isotopic homogeneity in the EM system, three new single-impact scenarios have been proposed. First, it has been suggested that the Moon-forming impact was a

hit-and-run event (Reufer et al., 2012) such that the impact could be characterized by more angular momentum than is currently present in the EM system, with the excess being carried off by the impacting body. Such an impact is capable of sourcing a somewhat higher percentage of the proto-lunar disk from Earth's mantle (~60%) than the standard scenario (~40%) and while this reduces the severity of the isotopic problem, it is unlikely to eliminate it entirely. Second, it has been suggested that the proto-Earth was rotating near the threshold for fission before the impact – with a < 3 hour rotation period – and that a high-velocity impactor struck it nearly head-on sourcing a satellite-forming disk directly from proto-Earth's mantle (Ćuk and Stewart, 2012). Finally, it has been proposed that the Moon-forming event may have been a nearly symmetric impact between two ~½ Earth-mass bodies (Canup, 2012). In such a scenario, both the emerging planet and the disk injected into circumplanetary orbit are sourced – by symmetry – equally from the two merging bodies. These last two scenarios have the potential to generate planet-satellite systems with close isotopic similarities, at least for the lithophile elements (Pahlevan, 2014). However, both scenarios generate planet-satellite systems with an overabundance of angular momentum – by a factor of 2 or greater – relative to the modern EM system. Hence, to be reconciled with the observed dynamical state of the EM system, most of the angular momentum in these systems must be transferred out. The only mechanisms known that might remove this amount of angular momentum from a planet-satellite system are the evection resonance (Ćuk and Stewart, 2012; Touma and Wisdom, 1998), a related limit cycle (Tian et al., 2017; Wisdom and Tian, 2015), or the Laplace plane instability (Atobe and Ida, 2007; Ćuk et al., 2016). The efficacy of these mechanisms, however, depends on specific values of the tidal dissipation parameters of the post-impact Earth and nascent Moon that are likely variable during this epoch in the crystallizing planet and satellite and not well-constrained. Magnetic winds have also been proposed as a way to carry off angular

momentum but the efficacy of this mechanism for the post-impact Earth-Moon system is also unclear (Gammie et al., 2016).

A different kind of solution to the problem of EM isotopic homogeneity – called equilibration – envisions a proto-lunar disk initially isotopically distinct from Earth, and invokes fluid dynamical mixing of the hot, convective, planet-disk system into a single isotopic reservoir during the ~10^3 years after the giant impact but before the cessation of lunar accretion (Pahlevan and Stevenson, 2007). Since the Moon accretes from the outermost disk material (Salmon and Canup, 2012), such a scenario requires that the proto-lunar disk undergo turbulent mixing across its radial extent. Efficient radial mixing is possible when the radial mixing timescale is short compared to the disk evolution timescale. Modeling the effect of turbulence on composition transport via a diffusivity D and the effect of turbulence on angular momentum transport via a viscosity ν, efficient radial mixing occurs when the turbulent Schmidt number Sc($\equiv\nu/D$) is much less than unity. Sc depends on the characteristics of disk turbulence. Although Sc has been measured in simulations of magnetically driven disk turbulence (Carballido et al., 2005), it has not yet been measured in simulations of the convectively driven turbulence that is likely present in the protolunar disk. The effective viscosity associated with convection is believe to be small (Lesur and Ogilvie, 2010; Stone and Balbus, 1996),

Given the suit of new ideas that have emerged aimed at understanding EM isotopic homogeneity and lunar origin more generally, we need new tools to discriminate between the various scenarios. Here, we describe development of one such tool. We show that turbulent radial mixing in a stratified proto-lunar disk – with a silicate vapor atmosphere and a separately convective magma

93 layer co-existing in equilibrium – makes specific predictions for mass-dependent isotopic offsets
94 in the composition of lunar and terrestrial silicates. We then use the measured isotopic abundances
95 to set constraints on how the proto-lunar disk could – and could not – have evolved. Finally, we
96 discuss implications for equilibration as the origin of the EM isotopic homogeneity.
97
98 **2. Disk Model**
99 Currently considered scenarios for a single Moon-forming giant impact (Canup, 2004, 2012;
100 Canup and Asphaug, 2001; Ćuk and Stewart, 2012; Reufer et al., 2012) shock heat and
101 disaggregate the lunar-forming material into a hot, melt-vapor circumterrestrial disk (Nakajima
102 and Stevenson, 2014). At present, no model exists that begins with such an initial state and follows
103 the evolution, ending with statements about the stable isotopic composition of the lunar-forming
104 material. Here, we describe a numerical disk model with the goal of forging a link between disk
105 processes and observable stable isotopic signatures. The physical picture envisioned for protolunar
106 disk evolution is similar to that initially envisioned for the equilibration hypothesis (Pahlevan and
107 Stevenson, 2007). The rationale for this choice is that developing the consequences of this scenario
108 can give rise to new tests and constraints on how Earth-disk equilibration could – and could not –
109 have occurred during the evolution of the proto-lunar disk.
110
111 2.1. Vertical structure
112 The melt-vapor disk generated by the giant impact settles into a nearly hydrostatic state – with a
113 vapor cloud expanding to assume a density distribution according to the local scale height – on
114 dynamical timescales of hours to days. Radiative cooling subsequently drives the evolution of the
115 proto-lunar disk. In the standard picture, vigorous turbulent convection is required to match high

116 radiative losses from a ~2,000 K photosphere (Thompson and Stevenson, 1988), above which the
117 thermal structure is determined by radiative transfer. Calculation of the disk vertical structure is
118 simplified by the fact that a negligible fraction of the atmospheric mass exists above the
119 photosphere (at ~millibar pressures) with the convective atmosphere extending down to pressures
120 of hundreds of bars (Thompson and Stevenson, 1988). The disk atmosphere is almost entirely
121 convective and, in analogy with planetary atmospheres, is expected to be characterized by an
122 adiabatic (or pseudoadiabatic) vertical structure (Holton, 1992).
123
124 A major unresolved question – which has consequences for lunar composition – is whether the
125 liquid in the proto-lunar disk exists as droplets kept in suspension via vigorous convective motions
126 (Thompson and Stevenson, 1988) or whether the liquid settles into a liquid-rich mid-plane layer
127 that dynamically decouples from the overlying atmosphere (Machida and Abe, 2004; Ward, 2012).
128 We refer to these two cases as the unstratified and stratified disks, respectively. An end-member
129 stratified disk scenario (herein called "fully stratified") is one in which, not only is the mid-plane
130 more liquid-rich than would be expected based on a single vertical disk isentrope, but the exchange
131 of matter between the convective liquid layer and the atmosphere is mediated by exchange of
132 atoms across a phase boundary, with no advective fluid motions carrying atoms directly between
133 the two layers (e.g. no convective overshoot). In such a fully stratified scenario, elements that
134 readily vaporize (e.g. O) will enter the atmosphere, and be available to undergo radial mixing and
135 isotopic equilibration (Pahlevan and Stevenson, 2007) while the more refractory elements (e.g. Ti)
136 will be concentrated in the mid-plane liquid layer and may undergo less Earth-disk equilibration.
137 EM isotopic heterogeneity for refractory elements has been sought, but not found (Zhang et al.,
138 2012).

Here, we assume that the disk is fully stratified: that the vertical structure consists of a convective liquid-rich mid-plane layer, a liquid-vapor interface, and an overlying convective atmosphere. The separately convective liquid-rich and vapor-rich columns are assumed to be in thermodynamic equilibrium at precisely defined interface conditions. Vertical mixing *within* each layer is assumed to be efficient because convective velocities are high and variations in atmospheric composition due to phase separation ("rainout") are expected to be small relative to the composition contrast between the liquid-rich layer and vapor-rich atmosphere (Pahlevan et al., 2011). Implications of relaxing the assumption of efficient vertical mixing are discussed in §4.2.

The pressure at the liquid-vapor interface is determined by hydrostatic balance with both the self-gravity of the disk and the vertical component of central planetary gravity:

$$-\frac{1}{\rho}\frac{\partial P}{\partial z} = 2\pi G\sigma(z) + \frac{GM_E}{r^3}z \qquad (1)$$

where ρ is the density, P is the pressure, z is the height above the mid-plane, G is the gravitational constant, $\sigma(z)$ is the local disk surface density enclosed at height z, M_E is the mass of the Earth, and r is the radial distance in cylindrical coordinates. This equation can be integrated to yield:

$$P_{\text{int}} = \frac{\pi G\sigma_T^2}{2}\left[1-(1-f_v)^2\right] + \frac{1}{2}\Omega^2\sigma_T f_v h_{mass} \qquad (2)$$

where P_{int} is the interface pressure, σ_T is the total surface density of the column (liquid layer plus atmosphere), f_v is the mass fraction of the vapor atmosphere in the column ($\equiv\sigma_v/\sigma_T$), Ω is the Keplerian angular velocity [$\equiv(GM_E/r^3)^{1/2}$], and h_{mass} is the mass-weighted scale height of the column which, for even moderate vapor fractions (f_v), can be approximated as the mass-weighted height of the vapor atmosphere:

$$h_{mass} = 2 \int_{z_{\text{int}} \approx 0}^{\infty} z \rho_v(z) dz \Big/ \int_{-\infty}^{\infty} \rho_v(z) dz \qquad (3)$$

We assume that the second term in equation (2) corresponding to the vertical component of Earth's gravity dominates, such that $h_{mass} \sim c_s/\Omega$, where c_s is the isothermal sound speed [$\equiv(kT/\mu)^{1/2}$] and μ the mean molecular weight of the vapor. By subsequently substituting nominal parameter values for the proto-lunar disk ($\sigma_T = 5\text{x}10^6$ g/cm^2, $\Omega = 2\text{x}10^{-4}$ s^{-1}, $c_s = 10^5$ cm/s) into both terms in equation (2), the dominance of the central gravity term in determining the disk vertical structure can be confirmed.[1] This calculation justifies neglecting the disk self-gravity, as also assumed in (Ward, 2012). Previous works have shown that the convective proto-lunar disk is nearly isothermal vertically due to the large latent heat of condensation of silicates in two-phase regions (Genda and Abe, 2003; Thompson and Stevenson, 1988). Accordingly, we adopt an isothermal vertical structure for the atmosphere with a well-known Gaussian density structure $\rho(z) = \rho(0)\exp(-z^2/H^2)$ and scale height given by $H = \sqrt{2}C_s/\Omega$. Substituting this structure into equation (3) yields a mass-weighted average height $h_{mass} = \sqrt{2/\pi}\ C_s/\Omega$, and substituting this expression into the second term in equation (2) yields an expression for the liquid-vapor interface pressure:

$$P_{\text{int}} = \frac{1}{\sqrt{2\pi}} f_v \sigma_T C_s \Omega \qquad (4)$$

We use this expression to relate the pressure at the liquid-vapor interface to other variables describing the state of the disk locally.

2.2. Radial structure

[1] Equivalently, one can check that Toomre's Q parameter ($c_{gas}\ \Omega$ / π G σ_{gas}) is >> 1, implying self-gravity is negligible.

180 The disks injected into orbit via giant impacts are generally compact disks, with most of the
181 orbiting mass confined to several planetary radii. For simplicity, here we assume that the surface
182 density profile characterizing the proto-lunar disk scales as ~1/r, as seen in simulations of the
183 standard impact (Canup et al., 2013). High angular momentum impacts (Canup, 2012; Ćuk and
184 Stewart, 2012) tend to create even more compact disks, which may cause identifiable differences
185 in the satellite that would result (Salmon and Canup, 2014). For the purpose of this work, we
186 neglect such differences in radial mass distribution. In order to make a connection between disk
187 process and isotopic observables, we assume that the proto-lunar disk extends from 1-5 Earth radii
188 (R_E) and that the outer disk material (extending from 3-5 R_E) accretes onto the Moon with its
189 isotopic composition expressed in the lunar samples, while the inner disk material (extending from
190 1-3 R_E) ultimately reaccretes back onto the Earth with its compositional character diluted and
191 essentially erased via mixing into the ~10^2x more massive terrestrial magma ocean. In reality, the
192 process of disk chemical evolution studied here and that of lunar accretion studied elsewhere
193 (Salmon and Canup, 2012) will overlap but any coupling between these processes is beyond the
194 scope of this work and must be subject to future modeling. Here, we restrict the study to
195 evolutionary disk processes that can cause the outer disk to acquire compositional characteristics
196 that are distinct from the inner disk, a distinctness that can be expressed in the composition of
197 silicate Earth and Moon. The initial thermal structure of the disk is taken to be radially isentropic:
198 simulations of impacts find that generated melt-vapor disks are composed of silicate materials that
199 experience similar levels of shock heating (Nakajima and Stevenson, 2014) and are therefore
200 approximately isentropic at the outset. Here, we adopt this initial state for calculations of the
201 subsequent thermochemical evolution.
202

2.3. Thermodynamic Model

We apply a 2-phase, 2-component thermodynamic model recently developed to study liquid-vapor fractionation in the aftermath of the giant impact (Pahlevan et al., 2011) to calculate equilibrium thermodynamic conditions (e.g. T, degree of vaporization) in the proto-lunar disk. The model has been previously described; here we summarize its features and describe its application to the proto-lunar disk. In brief, the silicate liquid is modeled as a binary solution of olivine end-members, $(Fe,Mg)_2SiO_4$, while the silicate vapor is described as a mixture of ideal gases consisting of gaseous species formed upon vaporization of such a liquid: SiO_2, SiO, Si, FeO, Fe, MgO, Mg, O_2, and O. This choice of compositional model is motivated by the fact that the bulk Moon – and therefore the proto-lunar disk – is known to be primarily composed of ferromagnesian silicates (Taylor and Wieczorek, 2014). At each time step in the evolution, we divide the proto-lunar disk into annuli and calculate thermodynamic equilibrium between the liquid layer and overlying vapor atmosphere. Input parameters for equilibrium calculations include the column entropy ranging from highly vaporized to fully condensed states (S=0.530-1.030 kJ/mol.K where mol refers to moles of olivine units or silicon atoms) and column composition (x_c=Fe/Fe+Mg), initially set equal to Earth mantle composition (≈0.1) (Jones and Palme, 2000). Using equations derived from the 2-phase equilibrium assumption (Pahlevan et al., 2011), as well as the pressure of equilibration (Equation 4), we solve for the interface temperature (T), the column vapor fraction (f_v), the specific entropy (S_L, S_V) and composition (X_L, X_V) of the liquid and atmospheric columns, as well as the partial pressure at the interface of each of nine vapor species (P_i) at each time step and annulus.

2.4. Radial transport

225 Because of the temperature-dependence of equilibrium partitioning (e.g. Eqn. 9), radial gradients
226 in interface temperature in the disk are expressed as radial gradients in composition of the liquid
227 layer and complementary atmosphere. Given that the disk atmosphere undergoes turbulent
228 convection (Thompson and Stevenson, 1988), the development of compositional gradients will
229 lead to transport of chemical and isotopic species down gradient. Hence, one consequence of an
230 equilibrium fully-stratified (settled liquid) disk model is the development of radial atmospheric
231 compositional gradients that – in concert with a convective, turbulently mixing atmosphere – will
232 lead to net radial transport of chemical and isotopic species. We assume that turbulent convection
233 in the disk atmosphere can be characterized by an eddy diffusivity (Tennekes and Lumley, 1972).
234 In the presence of atmospheric compositional gradients, atmospheric motions will then transport
235 species down gradient in accordance with Fick's law:

236 $$\vec{J}_{\mathrm{i}} = -\rho_v D_v \vec{\nabla} c_{i,v} \qquad (5)$$

237 where J_i [kg m^{-2} s^{-1}] is the mass flux of an atmospheric constituent *i*, ρ_v is the atmospheric mass
238 density, D_v is the turbulent diffusivity, and $c_{i,v}$ is the atmospheric mass fraction of constituent *i*. In
239 principle, a similar equation could be written for turbulent mixing in the magma layer. However,
240 because of both greater length scales and greater velocity scales associated with atmospheric
241 convection, convective radial transport is expected to be dominated by the atmospheric motions
242 (Pahlevan and Stevenson, 2007). Accordingly, we consider a liquid layer that is stationary but
243 which rapidly equilibrates with the overlying turbulent atmosphere. We take the divergence of
244 Eqn. (5), combining it with a continuity equation:

245 $$\frac{\partial\left(\rho_v c_{i,v}\right)}{\partial t} = -\vec{\nabla} \bullet \left(\rho_v D_v \vec{\nabla} c_{i,v}\right) \qquad (6)$$

to describe the atmospheric transport. Using the continuity equation here without sources or sinks is valid for species that are neither created nor destroyed in the atmosphere. Atomic abundances can therefore be described in this way, while molecular abundances cannot due to the occurrence of chemical reactions. Note that such an equation is only used to describe changes in the composition of the atmosphere and that compositional changes to the liquid layer arising from liquid-vapor equilibration are treated separately in the numerical model. The reason for this separate treatment is that – unlike signatures that are identical between a silicate liquid and co-existing vapor (e.g. $\Delta^{17}O$ studied in (Pahlevan and Stevenson, 2007)) – here we are considering chemical and isotopic signatures that are distinct between co-existing phases (e.g. $^{30}Si/^{28}Si$, see §2.6). Expecting rapid vertical mixing but rate-limiting radial mixing in the disk, we integrate Eqn. (6) vertically through the convective atmosphere:

$$\sigma_v \frac{\partial c_{i,v}}{\partial t} = -\vec{\nabla} \bullet \left(\sigma_v D_v \vec{\nabla} c_{i,v} \right) \quad (7)$$

where σ_v ($\equiv f_v \sigma_T$) is the atmospheric surface density [kg m^{-2}] and where we have assumed that this parameter has no time-dependence arising from disk turbulence. This assumption reflects the expectation that – while convective motions can drive the transport of species – turbulent convection leads to little or no net mass transfer. Indeed, numerical studies of disks have found that convection does not efficiently transport angular momentum (Lesur and Ogilvie, 2010; Stone and Balbus, 1996), a requirement for net mass transport. This issue is further discussed in §4.1. Atmospheric surface density does vary in our model due to thermal evolution (i.e. condensation, see §2.5). At each time step, we use Eqn. (7) in cylindrical coordinates to describe changes in atmospheric composition with no net flux boundary conditions, $\partial c/dr(R_E,t) = \partial c/dr(5R_E,t) = 0$. These boundary conditions reflect the simplification of neglecting moonlet formation and satellite-disk interactions in the outer disk (Salmon and Canup, 2012) and turbulent mixing with the silicate

vapor atmosphere of Earth in the inner disk (Pahlevan and Stevenson, 2007). Different boundary conditions are possible, but here we make this choice in order to interrogate processes within the proto-lunar disk itself, relegating interactions with its environment to future works.

2.5. Thermal evolution

It is well known that the viscous and thermal evolution of the proto-lunar disk is a closely coupled problem. As first pointed out by (Cameron and Ward, 1976), the material in the proto-lunar disk is susceptible to gravitational instability. These authors later calculated that the viscous evolution timescale for particles undergoing gravitational instability are of order ~1 year (Ward and Cameron, 1978). It was subsequently recognized that such a rapid evolutionary timescale would liberate enough gravitational energy for the material to self-vaporize, violating the original particle assumption (Thompson and Stevenson, 1988). Hence, the idea of a thermally regulated proto-lunar disk arose, whereby the heating due to viscous gravitational energy release would be matched by radiative losses in quasi-steady-state fashion. Accordingly, subsequent works explore coupled solutions to the viscous and thermal evolution (Charnoz and Michaut, 2015; Ward, 2012). Here, we adopt a simplified thermal history in which radiative losses are powered by secular cooling of the disk alone; we do not consider viscous heating. The motivation for, and limitations of, this assumption will be discussed in §4.1.

Treating radiative cooling as a quasistatic process, we can relate the outgoing heat and entropy fluxes using the thermodynamic identity, $dQ = TdS$, where T is the temperature of the radiated photons. Further approximating the radiation as a blackbody, we can write an expression for the entropy per unit area being radiated from both sides of the proto-lunar disk per unit time:

$$dS = 2\sigma_{SB} T_{ph}^{3} dt \quad (8)$$

where σ_{sb} is the Stefan-Boltzmann constant, T_{ph} is the photospheric temperature. We can use this expression to calculate radiative entropy losses from disk annuli as a function of time. Because of vertical convection, we expect the effects of radiative cooling to rapidly propagate down through the column; equivalently, the entire thermal reservoir of the disk can be tapped by radiative losses. At each time step, new values of entropy are derived for each annulus after radiative losses, while radial transport (§2.4) and liquid/atmosphere re-equilibration (§2.3) are calculated using an operator split scheme, i.e. calculating the effects of each process in sequence.

We follow the thermal evolution of the disk from an initial to a final state. Motivated by the impact simulations, we adopt initial thermal states for the proto-lunar disk – measured by the vapor fraction – ranging from mostly (~80%) liquid (Canup, 2004) to mostly (50-95%) vapor (Canup, 2012; Ćuk and Stewart, 2012). For final states, because we are interested in articulating expected compositions of the outer disk material, and because atmospheric transport is expected to dominate the radial transport over liquid-layer convection (§2.4), once the vapor in the outer disk (3-5 R_E) has nearly fully condensed ($f_v < 0.01$), the composition of the liquid is considered frozen-in, to be later expressed in the isotopic composition of the silicate Moon, i.e. of lunar samples. Hence, we consider the evolution of the disk until the outer disk has fully condensed. In addition to neglecting viscous heating, we do not consider turbulent radial transport of entropy and heat in the atmosphere, or other possible triggers of compositional freeze-in, e.g. disk fragmentation into moonlets, but discuss variations in disk models in §4.2 and §4.3.

2.6. Silicon isotopes as tracers

315 We choose to study the behavior of silicon isotopes as tracers for several reasons. First, it is known
316 that at sufficiently high temperature, equilibrium isotopic differences between co-existing phases
317 approach zero (Urey, 1947) and that small but significant isotopic fractionation is only possible at
318 high temperature where there are significant differences in bonding environment between the
319 phases present for the element under consideration. Silicon, for example, exists as SiO_4^{-4} in silicate
320 melts and predominantly as SiO in co-existing vapors (Visscher and Fegley, 2013), permitting
321 large liquid-vapor isotopic fractionation (~0.5 per mil in $^{30}Si/^{28}Si$) in the high-temperature
322 environment (~3,000-4,000 K) encountered during lunar origin (Pahlevan et al., 2011). Second,
323 unlike magnesium, iron, and oxygen, which significantly reside in multiple species in silicate
324 vapors, SiO dominates the vapor speciation of silicon (e.g. over SiO_2 and Si) for the full range of
325 conditions encountered in the proto-lunar disk (Visscher and Fegley, 2013). Because of such
326 simple vapor speciation, even a two-component thermodynamic model (§2.3) accurately captures
327 the speciation behavior for silicon in the actual proto-lunar disk, a requirement for accurately
328 articulating predictions of isotopic fractionation in scenarios of evolution. Finally, to forge a
329 connection with observables, we require an element whose isotopic composition in the bulk silicate
330 Earth and Moon are precisely known. Because the bonding environment for silicon in silicate melts
331 and co-existing crystals are rather similar (Huang et al., 2014), the silicon isotopic variations that
332 arise due to liquid-vapor fractionation are not encountered during ordinary (i.e. crystal-liquid)
333 petrologic processes (Zambardi et al., 2013). Accordingly, the isotopic composition of samples
334 reflects the process of liquid-vapor fractionation in the proto-lunar disk but not the subsequent
335 crystal-liquid geologic fractionations. Hence, the isotopic composition of the silicate Earth and
336 Moon can be derived from measurements on samples and are known to high precision, permitting

337 comparison of the observations with predictions of the post giant-impact evolution (Armytage et
338 al., 2012; Pahlevan, 2014).
339
340 Silicon isotopes are integrated as passive tracers into the model. At each time step, liquid-vapor
341 equilibrium at each annulus is characterized by a temperature, T (§2.3). Because the isotopic
342 fractionation is only a function of temperature in this low-pressure (<1GPa) system, we can
343 calculate the partitioning of Si isotopes between the silicate liquid and vapor as:

344 $$\Delta_{L-V} = 5 \times (10^3 / T)^2 \ \ per\ mil \qquad (9)$$

345 $$\delta_C = F_V^{Si} \delta_V + (1 - F_V^{Si}) \delta_L \qquad (10)$$

346 where $\Delta_{L\text{-}V}=\delta_L-\delta_V$ is the part per thousand difference of the $^{30}Si/^{28}Si$ between the liquid and vapor,
347 as previously calculated using standard procedures (Pahlevan et al., 2011) and δ_L, δ_V, δ_C represent
348 the isotopic compositions of the liquid layer, the vapor atmosphere and the entire column (liquid
349 layer plus atmosphere). We set the initial disk composition $\delta_C(r,0)$ to zero for reference. In this
350 way, one can calculate the radial isotopic structure of the proto-lunar disk atmosphere and liquid
351 layer, given a radial disk composition, $\delta c(r,t)$ and temperature structure, $T(r,t)$. Two features of the
352 isotopic partitioning are notable. First, $\Delta_{L\text{-}V}$ is positive, such that the heavier isotopes of silicon
353 will concentrate into the silicate liquids. Second, the temperature dependence of the fractionation
354 guarantees spatial variations in the liquid-vapor partitioning throughout the proto-lunar disk. In
355 particular, the radial gradient in equilibration temperature will be expressed – through equilibrium
356 partitioning (Eqn. 9) – as silicon isotopic gradients in the atmosphere and liquid layer. Once this
357 equilibrium state is calculated, we propagate the evolution forward by calculating the radial
358 isotopic transport via Eqn. (7), where $c_{i,v}$ now represents δ_V. After calculating radial transport, we
359 permit the atmosphere – now out of equilibrium with the underlying liquid layer – to re-equilibrate,

thereby changing the composition of the lunar-forming liquid. In this way, turbulent motions in the convective vapor atmosphere can change the isotopic composition of the nominally stationary Moon-forming liquid. In the case of silicon, such isotopic redistribution tends to concentrate the heavy isotopes in the outer (i.e. Moon-forming) regions of the disk.

3. Results

3.1. Thermal state and history

Because of the weak (logarithmic) dependence of the specific entropy of ideal gases with pressure, the initial isentropic state of the proto-lunar disk translates to a radially ~constant vapor fraction initially (Fig. 1a). Because of high latent heat of condensation and high vapor fractions (~tens of percent), the secular cooling heat budget of the proto-lunar disk is dominated by latent heat of condensation, with minor contributions from sensible heat ($c_p\Delta T$). Hence, unlike the post-impact atmosphere of Earth which is thermally buffered from below, secular cooling of the proto-lunar disk in the absence of viscous heating is rapid. Because of an outwardly decreasing surface density profile, the disk first cools at large distances with a condensation front that propagates inwards on a timescale of years (Fig. 1a).

The temperature structure of the disk has several notable features. First, even at the outset of the evolution, an isentropic disk is characterized by a significant radial temperature gradient, as also observed in (Nakajima and Stevenson, 2014). Second, because of more rapid cooling in the outer disk, the radial T-gradient of the disk steepens with time, ranging from 125-350 K/R_E (Fig. 1b). The existence of such a radial temperature gradient is expected to be a universal feature of any proto-lunar disk model and plays a central role in the evolution of isotopic signatures here studied.

383

384 3.2. Major element chemical fractionation

385 The 2-component [$(Fe,Mg)_2SiO_4$] thermodynamic model adopted has one variable for chemical
386 composition, x_{Fe}(≡Fe/Fe+Mg), rendering possible studies of chemical fractionation. Accordingly,
387 we track the x_{Fe} of the liquid, vapor, and total column in the proto-lunar disk during the evolution.
388 As has been experimentally determined, fayalite (Fe_2SiO_4) has a higher vapor pressure than
389 forsterite (Mg_2SiO_4) at identical temperature (Nagahara et al., 1994), a behavior clearly expressed
390 in the proto-lunar disk: the vapor atmosphere is enriched in FeO (x_{Fe}=0.12-0.35), while the liquid
391 layer is MgO-rich (x_{Fe}=0.02-0.06), relative to the composition of the column as a whole (x_{Fe}=0.1,
392 Fig. 2a). Moreover, due to the temperature and pressure gradients in the disk, even an initial radial
393 chemical homogeneity will – through equilibrium partitioning – result in radial chemical gradients
394 in liquid and atmospheric reservoirs. An increasing iron oxide content of the vapor atmosphere
395 with radius (Fig. 2a) implies an inward turbulent transport of iron in the atmosphere arising from
396 convective turbulence. Through liquid-vapor re-equilibration, atmospheric transport of species
397 also leads to the development of chemical gradients in the lunar-forming liquid. In this way,
398 turbulent transport can be expected to redistribute chemical species in the proto-lunar disk.

399

400 Two features of turbulent chemical transport are notable: (i) the outer disk material from which
401 the Moon forms is modestly depleted in iron-rich silicates relative to the inner disk, which falls
402 back onto Earth (Fig. 2b). The sign of this fractionation can be understood as follows: as the
403 outermost disk condenses, it becomes increasingly iron-rich (Fig. 2a), such that turbulent mixing
404 with the hotter, more highly vaporized inner disk depletes FeO from the lunar-forming material,
405 (ii) the magnitude of chemical fractionation is modestly dependent on initial disk vapor fraction

406 (Fig. 2b). This result can be understood since higher vapor fractions are associated with longer
407 secular cooling timescales (§3.1), permitting the chemical redistribution to proceed longer, and
408 since it implies a greater atmospheric mass (in which transport occurs) relative to the mass of the
409 melt layer, permitting more efficient turbulent transport and steeper chemical gradients to develop
410 per unit time. As expected, more vigorous turbulence results in greater chemical redistribution.
411 For the major elements here considered, the redistribution is small but non-negligible: for the range
412 of initial vapor fractions and turbulent diffusivities considered for the proto-lunar disk, the
413 resulting depletion in outer disk Fe/Fe+Mg is < 2x (Fig. 3). Hence, impact models that begin with
414 an Earth-mantle-like disk (Canup, 2012; Ćuk and Stewart, 2012) cannot generate an FeO-enriched
415 silicate Moon (Jones and Palme, 2000) via turbulent redistribution: some other process is required
416 (Pahlevan et al., 2011). Nevertheless, due to uncertainties in both the initial Fe/Fe+Mg in the proto-
417 lunar disk as well as in the lunar bulk chemical composition, modest chemical fractionation in the
418 proto-lunar disk is difficult to rule out using major elements. We conclude that the major element
419 composition of the Moon places modest constraints on chemical fractionation processes in the
420 proto-lunar disk.
421
422 3.3. Silicon isotope fractionation
423 Equilibrium silicon isotopic fractionation is significant, resulting in a ~0.4-0.5 per mil difference
424 in the $^{30}Si/^{28}Si$ of silicate liquids and vapors at the temperatures prevailing in the proto-lunar disk
425 (Fig. 4a). As discussed in §2.6, the proto-lunar liquid concentrates the heavy isotopes of silicon
426 while the complementary vapor atmosphere is isotopically light, with the difference between the
427 two reservoirs increasing with increasing radius, due to the negative radial temperature gradient
428 (Fig. 2b) and equilibrium partitioning law (Equation 9), which dictates enhanced fractionation at

lower temperatures. The resulting composition of the atmosphere exhibits greater isotopic lightness with increasing radial distance and implies an inward transport of light silicon isotopes accompanying turbulent convection in the atmosphere. Liquid-vapor equilibration transmits this signal to the proto-lunar liquid and the process continues until the proto-lunar disk has condensed and the isotopic structure has frozen in. As with chemical fractionation (§3.2), steeper gradients are generated from hotter initial states (Fig. 4b), the reasons being two-fold: longer cooling timescales and greater atmospheric masses causing greater transport and redistribution during the cooling history as a by-product of turbulent convection.

The magnitude of the silicon isotope fractionation is large relative to the precision with which the composition of terrestrial and lunar reservoirs is measured, permitting the development of a new stable isotopic constraint on the evolution of the proto-lunar disk. As in the case of chemical fractionation (§3.2), both more vigorous turbulence (higher α) and hotter initial thermal states result in greater isotopic fractionation between the outer (i.e. Moon-forming) and inner proto-lunar disk (Fig. 5). For nominal values of turbulent diffusivity ($\alpha=3\text{x}10^{-3}$), even modestly vaporized proto-lunar disks (f_v~0.2-0.4) can imprint measurable mass-dependent signatures onto the lunar forming material ($\delta^{30}Si_M$=0.05-0.1‰ – Fig. 5). An Earth-Moon isotopic offset of this magnitude can be excluded by existing observations (Armytage et al., 2012; Fitoussi and Bourdon, 2012). Possible interpretations of the data in light of the model results are discussed in §4.4.

4. Discussion

We have described a coupled thermochemical model for the evolution of the proto-lunar disk with the goal of forging a link between the stable isotopic composition of the lunar-forming material

452 and the parameters governing lunar disk evolution. Here, we discuss several simplifying features
453 of the adopted disk model, compare with other disk models discussed in the literature (§4.1-4.3),
454 and then consider the general conclusions that can be drawn about the evolution of the proto-lunar
455 disk using the model with constraints provided by the stable isotopic data (§4.4).
456
457 4.1. Viscous evolution
458 The model we have described neglects the viscous redistribution of mass and angular momentum
459 and the attendant gravitational energy release. Including viscous evolution into the disk model
460 would have several effects: (1) thermal: due to the depth of the terrestrial gravity well, significant
461 viscous spreading has significant thermal consequences; where viscous heating takes place, it can
462 easily dominate the heat budget of the melt-vapor column. For example, (Ward, 2012) described
463 a disk model characterized by a stratified melt-vapor structure with a viscous melt layer and an
464 inviscid atmosphere, and derived a cooling timescale for the proto-lunar disk of ~250 years, to be
465 compared with a cooling timescale of ~2 years for a f_v~0.2 disk powered by secular cooling alone
466 (§3.1). Hence, one consequence for the purely secular cooling powered disk model here described
467 is that the lifetime – and the magnitude of chemical and isotopic redistribution calculated for the
468 proto-lunar disk – are lower limits. The lifetime and degree of chemical fractionation is expected
469 to be greater in a model such as that described in (Ward, 2012), (2) transport/redistribution: viscous
470 dissipation causes outward (inward) transport of angular momentum (mass) and causes material
471 to spread radially, a flow that competes with turbulent mixing (Stevenson, 1990). Hence, by
472 neglecting the viscous evolution, we implicitly only consider diffusive ($D/\nu \geq 1$) transport regimes.
473 We have focused on this regime because it is in this regime in which extensive turbulent mixing
474 can take place (Pahlevan and Stevenson, 2007). However, even if a partially vaporized disk is

initially in the diffusive regime, it is possible that – as the disk condenses – it transitions to the viscous regime ($D/\nu \leq 1$) where radial mixing becomes inefficient. The calculations here presented only apply to redistribution in the diffusive regime.

4.2. Turbulent heat and entropy transport

We have considered turbulent transport in the presence of compositional gradients, but neglected the equivalent transport of heat in the presence of atmospheric entropy gradients. It is known that – in the presence of radial entropy gradients – a disk instability may arise at the expense of the entropy gradient ("radial convection") and thereby radially transport heat and entropy (Klahr and Bodenheimer, 2003; Lesur and Papaloizou, 2010). In the proto-lunar disk, such a radial entropy gradient may arise via preferential cooling or vertical phase separation of droplets ("rainout") in adjacent annuli of the proto-lunar disk. This process would have consequences for the calculations here presented: (1) thermal: since heat transport is outward, to the extent that this process takes place, it prolongs the thermal history and accentuates the chemical/isotopic signals that arise, and (2) compositional: since the effective gravity in the near-Keplerian disk is inwards, this process would also exchange vapor-rich (isotopically light) atmospheric parcels with more liquid-rich (isotopically heavy) parcels radially and may therefore moderate the magnitude of radial transport here calculated and soften the constraint here described. However, we see no reason to suppose that this effect would precisely cancel the isotopic fractionation based on the radial temperature gradient calculated in this work. In the absence of such a reason, the possibility of a fortuitous cancellation of two competing effects is considered unlikely. This issue needs to be investigated further.

498 4.3. Criterion for compositional freeze-in

499 While adopting initial conditions for disk evolution from the output of giant impact simulations is
500 straightforward, selecting a criterion for the cessation of disk evolution is less certain. Here, we
501 have considered a disk with chemical and isotopic redistribution but no net mass transport and no
502 fragmentation. In such a model, the condensation of the vapor atmosphere can be expected to halt
503 radial redistribution because the turbulent atmosphere is the agent that causes transport. However,
504 other criteria for compositional freezing of the disk are possible. (Canup et al., 2015) considered a
505 settled disk with a viscous liquid-rich midplane layer. In analogy with particle disks, the midplane
506 liquid layer was assumed to undergo gravitational instability and fragmentation to form moonlets
507 beyond the classical Roche radius at 2.9 R_E defined by lunar-density condensates. (Thompson and
508 Stevenson, 1988) instead considered a disk model in which a single vertical isentrope characterized
509 convective columns from the midplane up to the rarified regions where the disk atmosphere is
510 optically thin and radiative. In such a picture, radiative cooling in disk patches is balanced by
511 gravitational energy release until the material spreads to radii where this equality can no longer be
512 satisfied, at which point the patch instabilities lead to collapse and moonlet formation and the
513 composition of the moonlets is determined by the composition of the collapsing disk fragment
514 with constituent droplets and vapor. Regardless of the precise criterion for compositional freeze-
515 in for disk patches, it is clear that the liquid composition is effectively frozen-in once the vapor
516 atmosphere condenses. Moreover, satellite-disk interaction may also be important (Salmon and
517 Canup, 2012) but its coupling with the disk evolution must be relegated to future works.

518

519 4.4. Consequences for disk evolution and equilibration

520 We do not know – a priori – how the proto-lunar disk evolved. Here, we have considered a disk
521 model in which the liquid largely settles out into a liquid-rich layer that rapidly equilibrates with
522 the overlying atmosphere, with the turbulent diffusivity in the vapor atmosphere operating on a
523 shorter timescale than viscous dissipation in either the atmosphere (Carballido et al., 2016) or the
524 melt-rich layer (Ward, 2012). This is the same settling and transport regime originally envisaged
525 in the equilibration hypothesis (Pahlevan and Stevenson, 2007) and therefore provides constraints
526 on an evolutionary scenario of this kind. We have shown that in such a picture the proto-lunar disk
527 is expected to generate isotopic gradients that would be expressed as differences in the composition
528 of the silicate Earth and Moon. Such an Earth-Moon isotopic offset is not observed to a precision
529 of 30 ppm in the case of the silicon ($^{30}Si/^{28}Si$) (Armytage et al., 2012; Fitoussi and Bourdon, 2012).
530 In the light of the isotopic observations, the results of the modeling can be interpreted in four ways:
531 (1) imperfect settling: the proto-lunar liquid may fail to settle into a liquid-rich layer with a
532 separately convective atmosphere and instead, exchange between the midplane and vapor
533 atmosphere may be advective (e.g. convective overshoot), as also described in (Thompson and
534 Stevenson, 1988). In such a scenario, equilibration with the Earth would involve both a vapor
535 atmosphere as well as the suspended liquid droplets, and one would expect isotopic homogeneity
536 in the Earth-Moon system for all elements irrespective of volatility, (2) liquid-vapor equilibration:
537 we have assumed that liquid-vapor equilibration in this system is rapid relative to transport
538 timescales in the problem. While the vigor of convective motion makes this possible, the timescale
539 for liquid-vapor equilibration may depend on foam-physics at the liquid-vapor interface and is
540 therefore difficult to quantify. Hence, one interpretation of the silicon isotopic data is that the liquid
541 and vapor in the proto-lunar disk underwent phase separation into two distinct layers but did not
542 experience continuous and rapid chemical re-equilibration. While very large depletions of volatile

elements in the lunar material suggest that nearly all proto-lunar liquid equilibrated with some vapor, a timescale for liquid-vapor equilibration comparable to the evolutionary timescale cannot be ruled out, (3) other transport regimes: we have here restricted the discussion to transport regimes in which the total diffusivity is greater than the total viscosity ("the diffusive regime") such that mixing can outcompete disk spreading and homogenize the vapor atmosphere on a rapid timescale. This regime may be appropriate for a disk whose dominant instability is the convective instability, because convection in disks is known to produce turbulent mixing but weak angular momentum transport (Lesur and Ogilvie, 2010; Stone and Balbus, 1996). However, there exist other instabilities, e.g. the gravitational instability, that may entail different mixing and transport properties. Hence, it is also possible that the disk spent part of its evolution in the viscous regime not subject to the diffusive redistribution process here calculated, (4) high-temperature silicate thermodynamics: it is possible that a binary olivine thermodynamics does not accurately capture the vaporization behavior of silicon in the proto-lunar disk on which the modeling results are based. In particular, olivine is known to vaporize congruently (Nagahara et al., 1994) such that the degree of silicate vaporization and silicon vaporization are equivalent in an olivine thermodynamics. A more complex multi-component model need not display this behavior, rending silicon isotopes highly sensitive to the evolution of the proto-lunar disk for only a range of vapor fractions. The degree to which olivine thermodynamics accurately captures the vaporization behavior of any given element in the proto-lunar disk can be determined by development of more complex models of multi-component silicate melts at the temperatures (T=3,000-4,000 K) of relevance.

5. Conclusions

Recent isotopic observations on lunar and terrestrial samples strongly suggest that the lunar material is derived from the silicate Earth. While the disk stage of lunar evolution has been invoked to explain several features of the Earth-Moon system, including the high-precision isotopic homogeneity, a quantitative and observationally constrained description of proto-lunar disk evolution is lacking. Despite uncertainty in the initial thermal state, the settling and transport regimes, and the degree of thermal and chemical coupling to the post-impact Earth, it is well established that the proto-lunar disk experiences a two-phase (liquid-vapor) evolution. Here, we have developed a thermochemical scenario of disk evolution incorporating silicon isotopes as passive tracers. Our results demonstrate that silicon isotopic fractionation in the proto-lunar disk can be significant relative to the precision of existing measurements, yielding a new quantitative constraint on disk evolution. The principal conclusion of the model is that a "settled" proto-lunar disk in the diffusive regime would have developed isotopic offsets in the silicate EM system that are not observed. Hence, it is possible to use silicon isotopes to set constraints on Earth-disk equilibration: if system-wide turbulent mixing of the Earth-Moon system took place, it must have involved advective mixing of the proto-lunar liquid and the vapor atmosphere. Whether other disk evolutionary scenarios can be reconciled with the silicon isotopic homogeneity of the EM system must be subject to future studies. These results open a new quantitative window into the energetic aftermath of the Moon-forming giant impact.

Acknowledgements

This work was supported in part by the Poincaré Fellowship (K.P.) and in part by a grant from the Keck foundation. We acknowledge discussions with Dave Stevenson. We would like to dedicate this paper to the memory of Bill Ward, who pioneered the study of the proto-lunar disk.

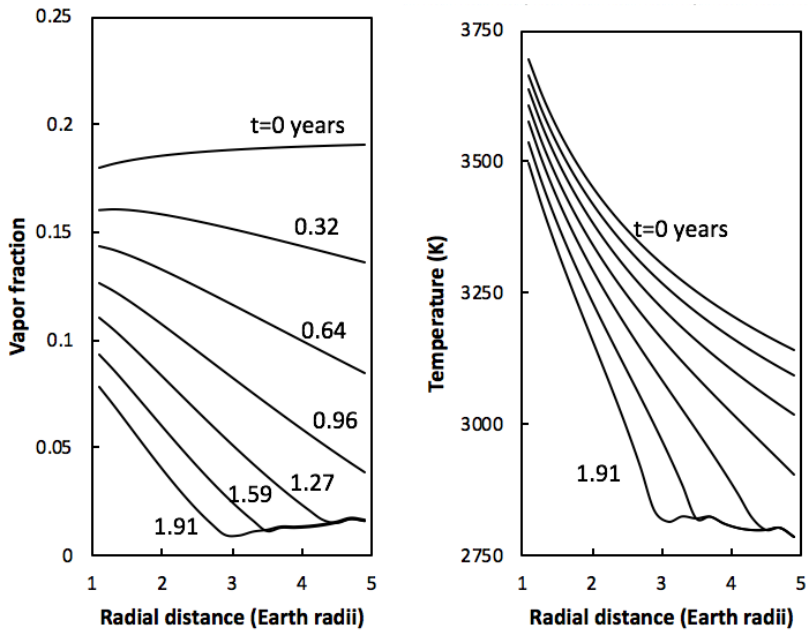

Figure 1. Disk thermal state and evolution. (a) Disk vapor fraction (atmospheric mass / total disk column mass) versus radial distance. This cooling history corresponds to an initial condition (f_v~0.2) generated via the "standard" impact. The simulations are halted at f_v~0.01 for numerical reasons. (b) Equilibration temperatures at the liquid-vapor interface versus radial distance. Note that, even in an initially isentropic disk, the disk is characterized by a radial temperature gradient due to the radial pressure gradient arising from e.g. radial surface density gradients in the disk, and cooling of the disk only accentuates a pre-existing T-gradients.

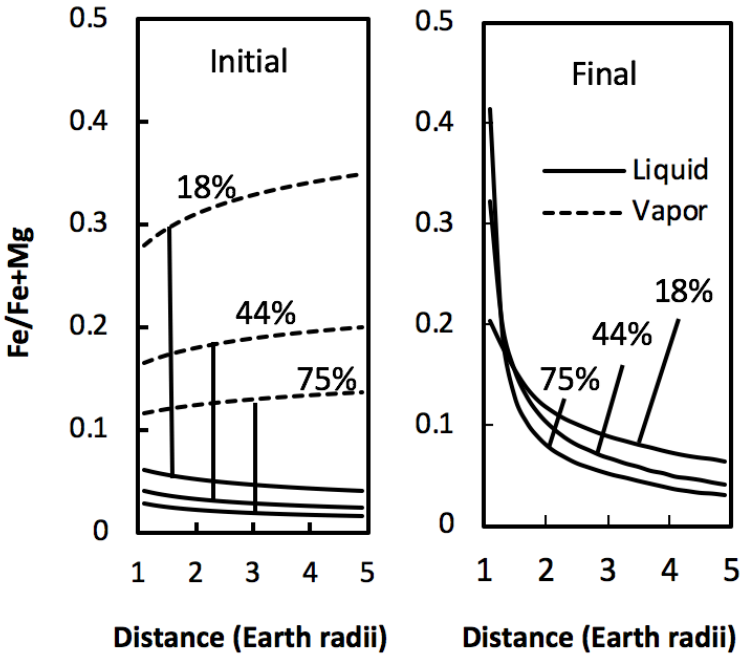

Figure 2. Fe/Mg redistribution in the proto-lunar disk. (a) Initial liquid-vapor partitioning in a disk with bulk x_{Fe}(Fe/Fe+Mg)=0.1. The percentage labels on curves correspond to initial disk vapor fraction. (b) Final compositional structure of the disk when the vapor has condensed and the liquid composition has frozen in. The vigor of turbulence in these simulations is $\alpha=3x10^{-3}$.

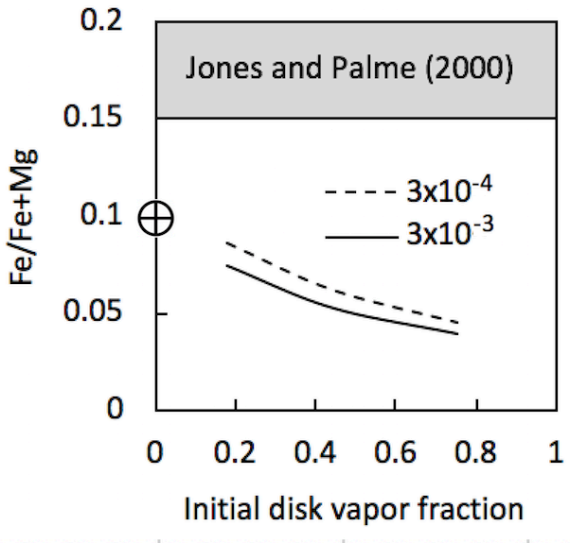

Figure 3. Summary of major element redistribution calculations. The curves represent final Fe/Fe+Mg of the outer (i.e. Moon-forming) disk after condensation versus the initial thermal state of the proto-lunar disk for two different values of the turbulent α parameter. Initial major element composition (i.e. Fe/Fe+Mg) of the disk is assumed to be the same in all cases ($\equiv$0.1), corresponding to a bulk silicate Earth initial composition. Non-zero turbulent diffusivity leads to redistribution of chemical species. While modest Fe/Fe+Mg variations can arise in the proto-lunar disk, the fractionation is of the wrong sign to produce the FeO enrichment of the bulk Moon, indicated by the shaded region).

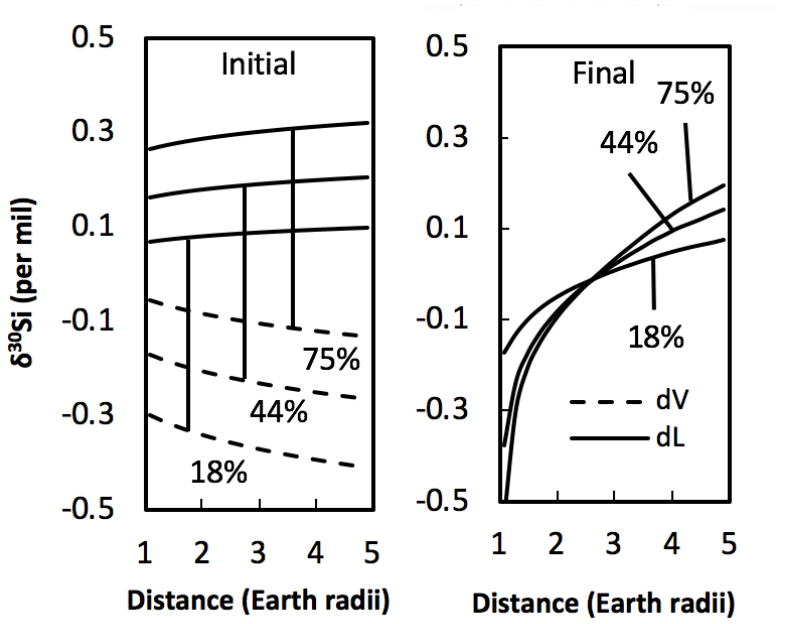

Figure 4. Silicon isotopic fractionation in the proto-lunar disk. (a) The initial radial isotopic structure of the proto-lunar disk atmosphere and liquid layer, with disks assumed to have a radially uniform initial composition set to zero for reference ($\delta^{30}Si=0$). The number labels on the curves correspond to the initial disk vapor fraction. Equilibrium partitioning leads to a liquid layer that is isotopically heavy with a complementary isotopically light atmosphere. (b) Final isotopic structure of the disk at the end of the thermal history when the vapor has condensed and the liquid composition has frozen in. The increasing isotopic lightness of the vapor atmosphere with radius implies in an inward transport of light isotopes whose magnitude depends on the disk initial vapor fraction.

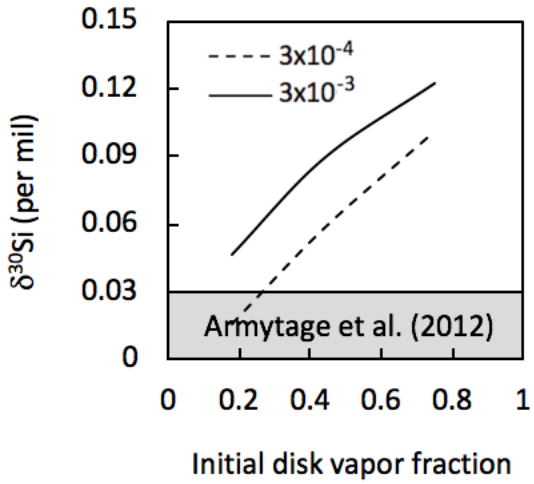

Figure 5. Summary of silicon isotopic redistribution in the proto-lunar disk. The average isotopic composition of the outer Moon-forming disk (3-5R_E) is plotted as a function of the initial vapor fraction for two different values of the turbulent α parameter. The initial composition of the disk ($\delta^{30}Si$) is set to zero in these calculations for reference. In the absence of radial diffusivity, the final and initial composition of the outer disk would be identical, but for even modest levels of turbulence, measurable isotopic differences between the inner and outer disk can evolve. Measurements on terrestrial and lunar samples observe no $\delta^{30}Si$ difference between the Earth and Moon ($\Delta^{30}Si$-EM=$\delta^{30}Si_E$-$\delta^{30}Si_M$) at a precision of < 0.03 per mil (Armytage et al., 2012; Fitoussi and Bourdon, 2012). Possible interpretations are discussed in §4.

588 **References**

589 Armytage, R.M.G., Georg, R.B., Williams, H.M., Halliday, A.N., 2012. Silicon isotopes in lunar
590 rocks: implications for the Moon's formation and early history of the Earth. Geochimica Et
591 Cosmochimica Acta, In Press.
592 Atobe, K., Ida, S., 2007. Obliquity evolution of extrasolar terrestrial planets. Icarus 188, 1-17.
593 Cameron, A.G.W., Ward, W.R., 1976. The origin of the Moon. Lunar Sci. 7, 120-122.
594 Canup, R.M., 2004. Simulations of a late lunar-forming impact. Icarus 168, 433-456.
595 Canup, R.M., 2012. Forming a Moon with an Earth-like Composition via a Giant Impact. Science
596 338, 1052-1055.
597 Canup, R.M., Asphaug, E., 2001. Origin of the Moon in a giant impact near the end of the Earth's
598 formation. Nature 412, 708-712.
599 Canup, R.M., Barr, A.C., Crawford, D.A., 2013. Lunar-forming impacts: High-resolution SPH and
600 AMR-CTH simulations. Icarus 222, 200-219.
601 Canup, R.M., Visscher, C., Salmon, J., Fegley Jr, B., 2015. Lunar volatile depletion due to
602 incomplete accretion within an impact-generated disk. Nature Geosci 8, 918-921.
603 Carballido, A., Desch, S.J., Taylor, G.J., 2016. Magneto-rotational instability in the protolunar disk.
604 Icarus 268, 89-101.
605 Carballido, A., Stone, J.M., Pringle, J.E., 2005. Diffusion coefficient of a passive contaminant in a
606 local MHD model of a turbulent accretion disc. Monthly Notices of the Royal Astronomical Society
607 358, 1055-1060.
608 Charnoz, S., Michaut, C., 2015. Evolution of the protolunar disk: Dynamics, cooling timescale and
609 implantation of volatiles onto the Earth. Icarus 260, 440-463.
610 Ćuk, M., Hamilton, D.P., Lock, S.J., Stewart, S.T., 2016. Tidal evolution of the Moon from a high-
611 obliquity, high-angular-momentum Earth. Nature 539, 402-406.
612 Ćuk, M., Stewart, S.T., 2012. Making the Moon from a Fast-Spinning Earth: A Giant Impact
613 Followed by Resonant Despinning. Science 338, 1047-1052.
614 Fitoussi, C., Bourdon, B., 2012. Silicon Isotope Evidence Against an Enstatite Chondrite Earth.
615 Science 335, 1477-1480.
616 Gammie, C.F., Liao, W.-T., Ricker, P.M., 2016. A Hot Big Bang Theory: Magnetic Fields and the
617 Early Evolution of the Protolunar Disk. The Astrophysical Journal 828, 58.
618 Genda, H., Abe, Y., 2003. Modification of a proto-lunar disk by hydrodynamic escape of silicate
619 vapor. Earth Planets and Space 55, 53-57.
620 Hartmann, W.K., Davis, D.R., 1975. Satellite-sized planetesimals and lunar origin. Icarus 24, 504-
621 515.
622 Holton, J.R., 1992. An Introduction to Dynamic Meteorology. Academic Press, San Diego.
623 Huang, F., Wu, Z., Huang, S., Wu, F., 2014. First-principles calculations of equilibrium silicon
624 isotope fractionation among mantle minerals. Geochimica et Cosmochimica Acta 140, 509-520.
625 Jones, J.H., Palme, H., 2000. Geochemical constraints on the origin of the Earth and Moon, in:
626 Righter, K., Canup, R.M. (Eds.), Origin of the Earth and Moon. University of Arizona Press, Tucson,
627 AZ, pp. 197-216.
628 Klahr, H.H., Bodenheimer, P., 2003. Turbulence in Accretion Disks: Vorticity Generation and
629 Angular Momentum Transport via the Global Baroclinic Instability. The Astrophysical Journal 582,
630 869.

631 Kruijer, T.S., Kleine, T., 2017. Tungsten isotopes and the origin of the Moon. Earth and Planetary
632 Science Letters 475, 15-24.
633 Lesur, G., Ogilvie, G.I., 2010. On the angular momentum transport due to vertical convection in
634 accretion discs. Monthly Notices of the Royal Astronomical Society: Letters 404, L64-L68.
635 Lesur, G., Papaloizou, J.C., 2010. The subcritical baroclinic instability in local accretion disc
636 models. Astronomy & Astrophysics 513, A60.
637 Machida, R., Abe, Y., 2004. The evolution of an impact-generated partially vaporized
638 circumplanetary disk. Astrophysical Journal 617, 633-644.
639 Nagahara, H., Kushiro, I., Mysen, B.O., 1994. Evaporation of Olivine - Low-Pressure Phase-
640 Relations of the Olivine System and Its Implication for the Origin of Chondritic Components in the
641 Solar Nebula. Geochimica Et Cosmochimica Acta 58, 1951-1963.
642 Nakajima, M., Stevenson, D.J., 2014. Investigation of the initial state of the Moon-forming disk:
643 Bridging SPH Cross Mark simulations and hydrostatic models. Icarus 233, 259-267.
644 Pahlevan, K., 2014. Isotopes as tracers of the sources of the lunar material and processes of lunar
645 origin. Philosophical Transactions of the Royal Society a-Mathematical Physical and Engineering
646 Sciences 372.
647 Pahlevan, K., Morbidelli, A., 2015. Collisionless encounters and the origin of the lunar inclination.
648 Nature 527, 492-494.
649 Pahlevan, K., Stevenson, D.J., 2007. Equilibration in the aftermath of the lunar-forming giant
650 impact. Earth and Planetary Science Letters 262, 438-449.
651 Pahlevan, K., Stevenson, D.J., Eiler, J.M., 2011. Chemical fractionation in the silicate vapor
652 atmosphere of the Earth. Earth and Planetary Science Letters 301, 433-443.
653 Reufer, A., Meier, M.M.M., Benz, W., Wieler, R., 2012. A hit-and-run giant impact scenario. Icarus
654 221, 296-299.
655 Salmon, J., Canup, R.M., 2012. Lunar Accretion from a Roche-Interior Fluid Disk. Astrophysical
656 Journal 760.
657 Salmon, J., Canup, R.M., 2014. Accretion of the Moon from non-canonical discs. Philosophical
658 Transactions of the Royal Society a-Mathematical Physical and Engineering Sciences 372.
659 Stevenson, D.J., 1990. Chemical Heterogeneity and Imperfect Mixing in the Solar Nebula.
660 Astrophysical Journal 348, 730-737.
661 Stone, J.M., Balbus, S.A., 1996. Angular momentum transport in accretion disks via convection.
662 Astrophysical Journal 464, 364-372.
663 Taylor, G.J., Wieczorek, M., 2014. Lunar bulk chemical composition: a post-Gravity Recovery and
664 Interior Laboratory reassessment. Philosophical Transactions of the Royal Society a-
665 Mathematical Physical and Engineering Sciences 372.
666 Tennekes, H., Lumley, J.L., 1972. A First Course on Turbulence. The MIT Press, Cambridge,
667 Massachusetts.
668 Thompson, C., Stevenson, D.J., 1988. Gravitational-Instability in 2-Phase Disks and the Origin of
669 the Moon. Astrophysical Journal 333, 452-481.
670 Tian, Z., Wisdom, J., Elkins-Tanton, L., 2017. Coupled orbital-thermal evolution of the early Earth-
671 Moon system with a fast-spinning Earth. Icarus 281, 90-102.
672 Touma, J., Wisdom, J., 1998. Resonances in the early evolution of the earth-moon system.
673 Astronomical Journal 115, 1653-1663.

Urey, H.C., 1947. The Thermodynamic Properties of Isotopic Substances. Journal of the Chemical Society, 562-581.
Visscher, C., Fegley, B., 2013. Chemistry of Impact-Generated Silicate Melt-Vapor Debris Disks. Astrophysical Journal Letters 767.
Ward, W.R., 2012. On the Vertical Structure of the Protolunar Disk. Astrophysical Journal 744.
Ward, W.R., Cameron, A.G.W., 1978. Disc Evolution Within the Roche Limit, Lunar and Planetary Science Conference IX, Houston, Texas.
Ward, W.R., Canup, R.M., 2000. Origin of the Moon's orbital inclination from resonant disk interactions. Nature 403, 741-743.
Wisdom, J., Tian, Z.L., 2015. Early evolution of the Earth-Moon system with a fast-spinning Earth. Icarus 256, 138-146.
Zambardi, T., Poitrasson, F., Corgne, A., Meheut, M., Quitte, G., Anand, M., 2013. Silicon isotope variations in the inner solar system: Implications for planetary formation, differentiation and composition. Geochimica Et Cosmochimica Acta 121, 67-83.
Zhang, J.J., Dauphas, N., Davis, A.M., Leya, I., Fedkin, A., 2012. The proto-Earth as a significant source of lunar material. Nature Geoscience 5, 251-255.